Infrared Physics and Technology 97 (2019) 1–5

Contents lists available at ScienceDirect

Infrared Physics & Technology

journal homepage: www.elsevier.com/locate/infrared

Regular article

Phase-matching in KTP crystal for THz wave generation at room temperature and 81 K

Chun-Rui Wang[a,b], Qi-Kun Pan[a,b], Fei Chen[a,b,*], Grigory Lanskii[c], Nazar Nikolaev[d], Alexander Mamrashev[d], Yury Andreev[c,e], Arkadii Meshalkin[f]

[a] State Key Laboratory of Laser Interaction with Matter, Changchun Institute of Optics, Fine Mechanics and Physics, CAS, Changchun 130033, China
[b] Innovation Laboratory of Electro-Optical Countermeasures Technology, Changchun Institute of Optics, Fine Mechanics and Physics, CAS, Changchun 130033, China
[c] Institute of Monitoring of Climatic and Ecological Systems, SB RAS, 10/3, Akademicheskii Ave., Tomsk 634055, Russia
[d] Institute of Automation and Electrometry, SB RAS, 1, Ac. Koptyug Ave., Novosibirsk 630090, Russia
[e] Siberian Physical–Technical Institute of Tomsk State University, 1, Novosobornaya Sq., Tomsk 634050, Russia
[f] Institute of Thermophysics, SB RAS, 1, Ac. Lavrent'ev Ave., Novosibirsk 630090, Russia

ARTICLE INFO

Keywords:
KTP
Nonlinear crystal
Optical properties
Harmonic generation
Frequency mixing

ABSTRACT

Optical properties of high-quality flux-grown potassium titanyl phosphate ($KTiOPO_4$, KTP) crystals were studied at 81 K in the spectral range of 0.2–2.4 THz by terahertz time-domain spectroscopy and compared with the room temperature results. No strong phonon peaks were found at frequencies below 2.15 THz in the absorption spectra of $\alpha_x \approx \alpha_y$ components. At 81 K they do not exceed that of widely used GaSe crystal. Experimental data on the dispersion of refractive index at 81 K for THz waves polarized parallel to optical axes were approximated in the form of Sellmeier equations. Phase matching for collinear difference-frequency generation of visible and near-IR emission into the THz domain was found possible, as well as second harmonic generation within THz region that can be a basis for the new THz sources designs. Phase matching in KTP was found insensitive to temperature variation. These properties together with the exceptional set of other known physical properties render KTP crystal amongst the most prospective crystals for high-power THz wave generation under intense laser pumping.

1. Introduction

Positive ($n_x < n_y < n_z$, $2V_z = 37.4°$ at $\lambda = 0.5461$ μm) potassium titanyl orthophosphate $KTiOPO_4$ crystal (hereafter KTP) belonging to the point group symmetry *mm2* is a widespread nonlinear crystal for frequency conversion. It is due to its exceptional optical properties: a broad transparency window between 0.35 and 4.5 μm at "0″ level, low (down to and below 10^{-3} cm^{-1}) absorption coefficient in the spectral range from 1.0642 μm to 1.318 μm, large birefringence of 0.11, high damage threshold of over 30 GW/cm^2 under expose to 8–11 ns pulses at 1.064 μm that is something lower to that for $LiNbO_3$ crystal, reasonable hardness (5 in the Mohs scale) and nonlinear coefficients ($d_{15} = 1.9$ pm/V, $d_{24} = 4.2$ pm/V, $d_{31} = 2.2$ pm/V, $d_{32} = 2.7$ pm/V, and $d_{33} = 17.4$ pm/V) [1]. KTP also demonstrates a low thermal expansion coefficient and slow variation of the optical constants with temperature (excellent thermal stability) [2], and high chemical stability [3]. It should be noted that absorption losses in KTP are significantly dependent on the growth technology (hydrothermal synthesis or flux method) and technological state of the art [1].

The assignment between the dielectric and crystallographic axes for KTP is ***X***, ***Y***, ***Z*** → ***a***, ***b***, ***c***. Phase matching (PM) exist in KTP for sum frequency (SFG) and second harmonic generation (SHG) within transparency window at room temperature (RT) by type II of three-wave interaction: f + s → f (e + o → e) type in the principle ***XY***-plane, f + s → s (o + e → o) in the ***YZ***-plane and f + s → f (o + e → o) in the ***XZ***-plane ($\theta > V_z$). Conventional notation of interacting waves in biaxial ("f" is a fast wave, "s" is a slow wave) and uniaxial ("o" is ordinary wave and "e" is extraordinary wave) crystals are used here for convenience [3]. The efficient nonlinear coefficient for type I PM is vanishing for interactions in ***XY***- and ***YZ***-plane; it is small for interaction in the ***XZ***-plane [4]. Difference-frequency generation (DFG), as well as optical parametric oscillation (OPO) were realized in KTP [4,5] demonstrating the highest efficiency in the ***XZ***-plane [5,6].

Introduction of time-domain terahertz spectroscopy (THz-TDS) has made it possible to measure KTP absorption coefficient α_y and α_z and refractive index n_y and n_z components in the range from 0.2 THz to

* Corresponding author at: State Key Laboratory of Laser Interaction with Matter, Changchun Institute of Optics, Fine Mechanics and Physics, CAS, Changchun 130033, China.
E-mail address: feichenny@126.com (F. Chen).

https://doi.org/10.1016/j.infrared.2018.12.012
Received 16 September 2018; Received in revised form 6 December 2018; Accepted 8 December 2018
Available online 10 December 2018
1350-4495/

1 THz for waves polarized parallel to ***Y***- and ***Z***-axis, respectively [7]. Unidentified component (it seems that wave polarization was not selected) was measured in the range of 0.5–2 THz [8]. All three components of the refractive index and absorption coefficient were measured between 0.2 and 2.6 THz for the first time in [9]. It was found that KTP exhibits strong birefringence $B = n_x - n_y \approx 0.65$ in the frequency range of 0.3–1.5 THz at RT and the pronounced absorption coefficient $\alpha_z \leq 50\,cm^{-1}$. Absorption coefficients $\alpha_x \approx \alpha_y = 15\,cm^{-1}$ at 1.5 THz and decrease down to $\sim 2\,cm^{-1}$ at longer wavelengths [9]. So, absorption coefficients α_x and α_y of KTP have the close values to GaSe [10]. Thus, KTP can be considered as a highly prospective crystal for THz applications on the level with widely used GaSe [11]. It was already used as the nonlinear medium in a surface-emitted terahertz-wave OPO [12–14]. Terahertz parametric generation from KTP was reported to be superior over lithium niobate ($LiNbO_3$) and lithium tantalate ($LiTaO_3$) in terms of parametric gain and laser damage resistance [13]. Besides, further improvement in the growth technology [9] or/and cooling [15,16] can significantly decrease its optical losses. So, KTP abundantly satisfies all requirements and therefore appears to be a highly attractive candidate for THz wave generation. To uncover the full potential of KTP crystals for the THz range it is necessary to carefully determine corresponding optical properties and a possibility for phase-matched generation at RT and lower temperatures that can be resulted in decreased absorption coefficient like in $LiNbO_3$ and/or more favorable PM conditions, and finally in improved frequency conversion efficiency.

Terahertz optical properties of high optical quality flux-grown KTP crystals studied by THz-TDS at 81 K are reported in this paper and compared with the RT results. Dispersions of refractive index components for THz waves polarized parallel to the optical axis are approximated in the form of Sellmeier equations; PM curves for difference-frequency generation in the THz domain (T-DFG) under visible and near-IR pump, and SHG within THz range were demonstrated in our previous work [17] but here we consider one more possible type of interactions for the same frequency conversion processes.

2. Materials and methods

A modified Czochralski method was employed by Single Crystals LLC, Russia (same crystal producer as for former study [10]) to grow a KTP ingot by flux method in a gradient temperature field with using a seed crystal oriented along the ***X***-axis. Vibrational methods of viscosity measurements and phase analysis were used to control melt characteristics and crystallization parameters. It allowed us choosing optimal flux composition and optimum process regimes for growing large ($> 250\,cm^3$) ingots with higher growth speed and specific resistance of up to $(2–4)\cdot10^{11}$ Ohm·cm at RT [18].

For biaxial crystal measurement of the α_x, α_y, α_z and n_x, n_y, n_z components is carried out for waves incident along the normal to the surface and polarized parallel to the optical axes ***X***,***Y*** or **Z**. Two high-resistivity at RT (10^{11} Ohm·cm) wafers with the size of about $10 \times 10 \times 0.275\,mm^3$ (width × height × thickness) were cut from the grown ingot orthogonal to ***X***- (KTP_x wafer) and **Z**-axes (KTP_z wafer) (Fig. 1).

The wafer's sides were cut, respectively, parallel to ***Y***- and ***Z***-axes, and ***X***- and ***Y***-axes (Fig. 1). So, as mentioned above, they allowed us to measure all three components of refractive index (n_x, n_y, and n_z) and absorption coefficient (α_x, α_y, and α_z). Possible nonparallelism of optical axis and light polarization caused by manufacturing mistake or misalignment of the optical setup leads to an appearance of an orthogonally polarized light component and, as a result, to the observation in the spectrum of an interference pattern. The coincidence of the optical axis and polarization of the THz waves was controlled by grid polarizers.

A spectrometer Cary 5000 Scan (Varian, Australia) with operation range of 190–3500 nm, spectral resolution of 0.2 nm and a Fourier spectrometer FT-801 (Simex, Russia) with operation range of 2–20 μm and spectral resolution of $0.5\,cm^{-1}$ were used to study absorption spectra in the main transparency window of the crystal. A custom-made THz-TDS (Fig. 2) was used to record optical properties of the KTP wafers in the THz domain.

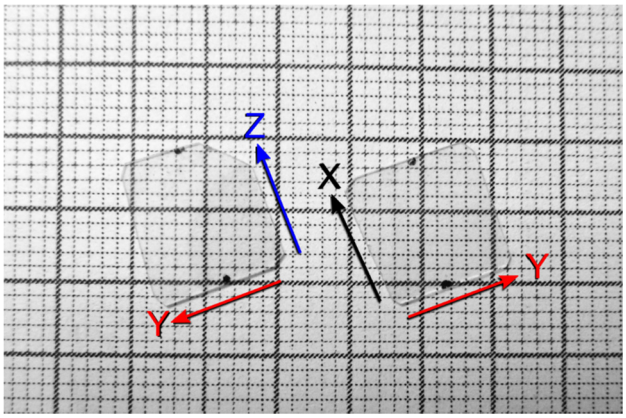

Fig. 1. Photo of the KTP wafers identified in the figure insets; their optical axes are shown by arrows.

It was based on a compact femtosecond 130-fs Er-doped fiber laser combined with an SHG module (Toptica Photonics, Germany), which delivers the average power of 80 mW at 775 nm. Laser radiation was split into two beams. About 90% of the power was used to pump a THz generator - an interdigitated high power multi-slit dipole antenna iPCA – 21–05 – 1000–800-h (Batop GmbH, Germany). About 10% of the power was utilized to probe the THz electric field by a conventional electro-optical sampling technique based on Pockels effect [19,20]. The emitted THz waves were collimated into the beam with a diameter of about 25 mm by an off-axis parabolic mirror and then focused by a similar mirror onto the detector: (1 1 0)-cut 2-mm thick antireflection coated ZnTe crystal. A voltage generator modulates the output THz radiation at $f_{mod} = 8$ kHz by switching the antenna's bias voltage (± 15 V). The lock-in amplifier SR830 (Stanford Research Systems, USA) was used to detect the THz signal at f_{mod}. The custom-developed software records the waveform of THz pulses by controlling the optical delay line and an output signal of the lock-in amplifier. The developed THz-TDS operated in the spectral range of from 0.1 to 2.5 THz, while its dynamic range exceeds 75 dB at the frequency of 0.3 THz.

A TPX lens with 100 mm focus lengths was used to focus the THz radiation onto the sample mounted inside the cryostat and then an identical second lens collimates it. The THz radiation was linearly polarized by P1 and P2 grid polarizers located, respectively, on the generator output and before the detector input. The fine-tuning of the spectrometer polarization optics was performed before the studies by the algorithm described elsewhere [21]. The THz-TDS signals were acquired with the time resolution of 125 fs in the range of 60 ps that corresponds to the spectral resolution of about 20 GHz. Since THz-TDS technique is differential one the records of THz pulse waveforms with (sample pulse) and without (reference pulse) sample are required to obtain the properties of the material under the study. The terahertz optical properties and thickness of the samples were estimated by the extraction method described in [22] and based on the complex transmission function calculated as the ratio of the Fourier-transform spectra of the sample and the reference pulses. The resulting complex transmission functions were averaged over four independent measurements.

A custom-made liquid nitrogen (LN) bath cryostat operating in a transmission mode and mounted on the translation stage was used to cool down the KTP wafers. Heating up and cooling down procedures are necessary for sample removing in the case of conventional cryostat technique. Thus, it can take more than an hour between the records of the sample and the reference THz pulses. As a result, an additional uncertainty can be introduced in complex transmission function due to

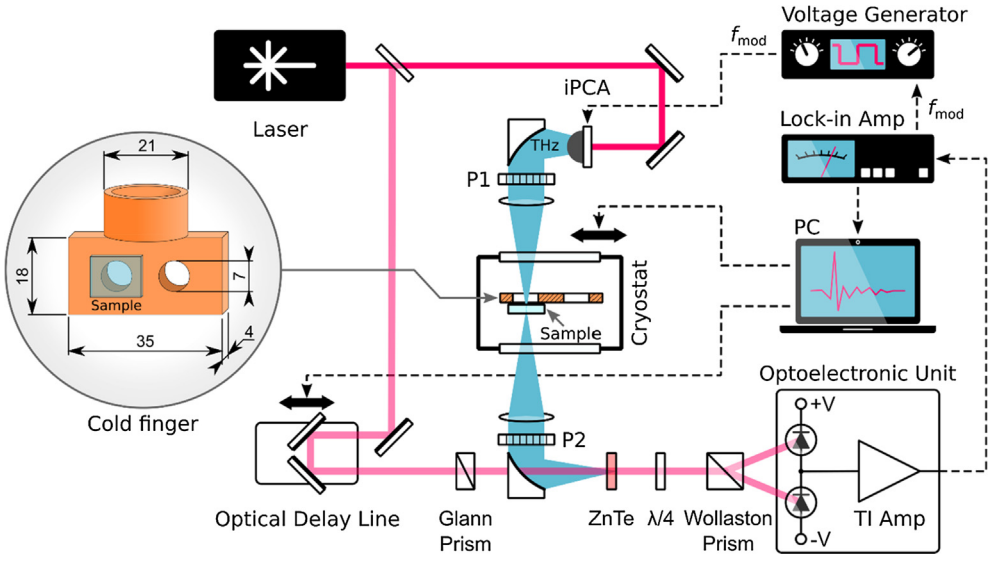

Fig. 2. Schematic of the THz-TDS: Magenta lines-laser radiation (775 nm, 130 fs, 80 mW); sky blue lines-THz radiation; black bold arrows indicate translation stage travel direction; dashed lines with arrows indicate electrical signals flow direction; P1, P2-terahertz grid polarizers; optoelectronic unit is based on the Si pin photodiodes and transimpedance amplifier. Cu custom-made cold finger (dimensions are in mm) is shown in the figure inset. (For interpretation of the references to colour in this figure legend, the reader is referred to the web version of this article.)

the long-term drift of the spectrometer signal amplitude. We made a special cold finger for our cryostat (Fig. 2 inset) to avoid this problem. A Cu cold finger was fabricated by CNS machine and has a symmetrical design with two identical windows. One of the diaphragms held the sample but the second one was free of the sample and used to measure the reference signal. The diaphragms interchangeably were exposed into the terahertz beam by moving the whole cryostat using a motorized translation stage. The wafer temperature was controlled by ANSI Type K (chromel-alumel) thermocouple integrated into the cold finger and connected to the calibrated "Termodat-13E1" temperature controller (Control Systems Co. Ltd., Russia). The spectral measurements on THz-TDS were performed after 30-minute settling time to the stable temperature of 81 K. We suggest that the difference in temperature between LN and wafer can originate from a big size of the cold finger and limited thermal insulation of the cryostat. However, new cold finger allowed us to perform more accurate studies of the THz optical properties of the KTP crystals than in former paper [9].

3. Results and discussion

The Fig. 3 plots absorption coefficient spectra (α_x, α_y, α_z) of the KTP wafers in the main transparency window at RT. All measured components of the absorption coefficient are below 0.1 cm^{-1} (lower limit of the measurement) that confirms the high optical quality of the wafers. It is seen in the Fig. 3 that KTP crystal permits pumping by a wavelength of 0.375–4.2 μm, i.e. blue-green, all solid state or chemical lasers. In particular, terawatt-level laser systems can be used as extreme power pump sources such as THL-100 generating 50-fs, 1–2 J pulses [23]. It comprises a driving Ti:Sapphire laser system (wavelength 950 nm, pulse energy 50 mJ), a frequency doubler and a second harmonic amplifier on excimer molecules XeF(C-A). Another possible pump source is a second harmonic of the 50-fs Ti:Sapphire "SART-248 M" system [24].

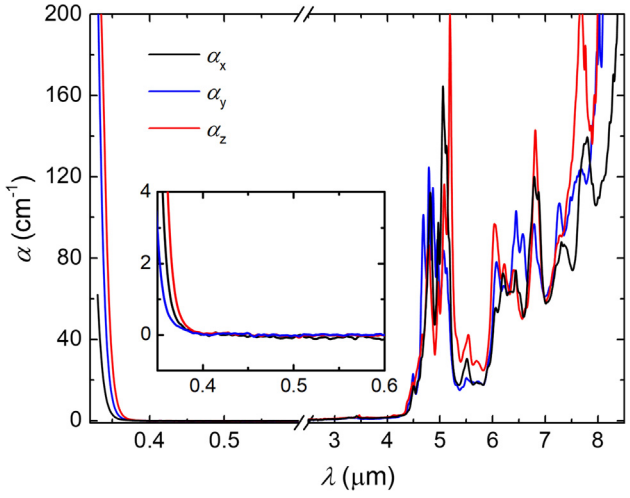

Fig. 3. Absorption coefficient spectra of the 0.275-mm thick KTP wafers in the visible and IR ranges at RT. Scaled up curves are shown in the figure inset (impossible to measure accurately due to the sensitivity limitations of the measuring system).

A non-centrosymmetric phase of KTP wafers at temperatures down to 81 K was confirmed by observation of SHG of 1.0642-μm Nd:YAG laser in a ***XZ***-slab cut of the same KTP ingot at θ (72°) > V_z (17.4°) during the cooling by adjusting it within an external angle of < 6°. Besides, it was found no major changes in THz spectra of the wafers with the cooling (see below) that could be related to the structural transformations.

Spectra of terahertz optical properties of KTP crystal measured by THz-TDS at 293 K and 81 K are depicted in the Fig. 4 and Fig. 5.

In Fig. 4 the refractive index components at 1 THz $n_z = 4.0$, $n_y = 3.35$ and $n_y = 3.3$, and birefringence $B = n_z - n_y \approx 0.7$ at RT match well with the data reported in [7]. All three components of the refractive index are a little bit larger than that are reported in [9]. At 81 K they decrease by less than 10% and seem still large enough for PM.

Similar to [25] refractive index components recorded at 81 K were approximated in the form of Sellmeier equations by the best-fit method within the validity range of 142–1500 μm:

$$n_x^2 = 9.07963 + \frac{1.20539\lambda^2}{\lambda^2 - 12497},\ n_y^2 = 9.20704 + \frac{1.36025\lambda^2}{\lambda^2 - 12264},\ n_z^2 = 11.8979 + \frac{2.36823\lambda^2}{\lambda^2 - 11336} \quad (1)$$

Along with the dispersion equations for the transparency window of flux-grown crystals and their thermal dispersions from [26] they were used to calculate PM curves for down-conversion into the THz domain.

PM for T-DFG under visible or near-IR pump was found possible all over the entire transparency range of KTP crystal in the THz domain including principle ***XZ*** plane ($\theta > V_z$ and $\theta < V_z$) both at 293 K and 81 K. An example of the calculated PM curves for T-DFG of Nd:YAG and close-wavelength OPO is shown in the Fig. 6 for 81 K and compared to 293 K. It is seen that PM curves are almost unchanged with the cooling that does not affect the T-DFG efficiency and well matches the data for

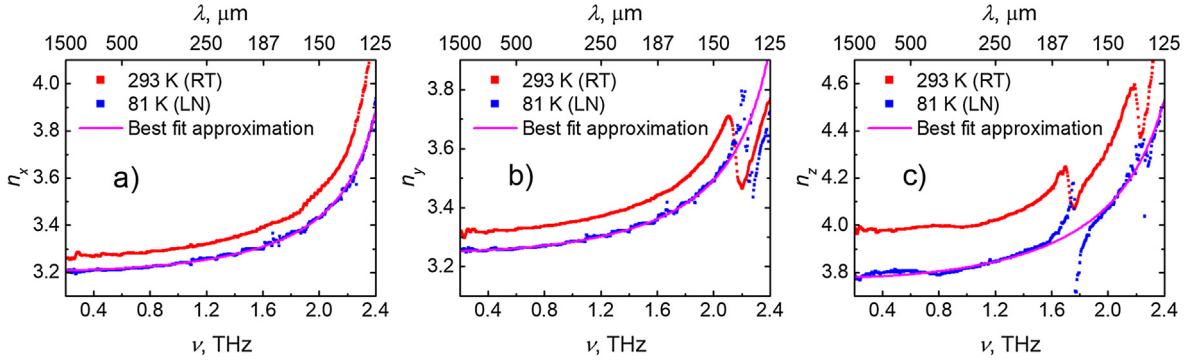

Fig. 4. Dispersion of refractive index of three axes of KTP crystal at 293 K and 81 K.

the main transparency window [1]. Pumping cm-sized KTP samples by extreme power visible or near-IR sources seems to be an attractive way to get top power nanosecond THz pulses.

It is interesting to outline that SHG within the THz domain was also found possible at 81 K as well as at RT (Fig. 7). Again, PM was found to be almost temperature insensitive. Thus, frequency conversion of THz waves can become an alternative design for new THz sources.

At RT absorption coefficient α_z is large (from 10 to 50 cm^{-1}) in the range between 0.5 and 1.5 THz (Fig. 5c), $\alpha_x \approx \alpha_y$ is 5 times lower than α_z (Fig. 5a, b) [9,25]. All of them decrease dramatically with the cooling down to 81 K leading to a significant increase in potential efficiency of T-DFG. Absorption coefficients α_x and α_y are close (about 5 cm^{-1}) to that of GaSe [10] and up to a few tens of cm^{-1} lower than that of $LiNbO_3$ [15] crystal at 1 THz. Phonon absorption peaks are found near 1.73 THz and 2.2 THz in α_z spectrum, 2.15 THz in α_y and 2.44 THz in α_x. No strong phonon peaks were found in α_x and α_y spectra at frequencies below 2.15 THz that also well matches known data [3,7,9,25,27,28].

Possible T-DFG in the ***XZ*** plane at $\theta > V_z$ is preferable due to lower absorption coefficient (Fig. 5). It should be noted that absorption coefficients can be further decreased by the improvement of the growth technology. Compared with LiB_3O_5 crystal [29–31] KTP crystal demonstrates an order larger nonlinearity and in comparison to $LiNbO_3$ it has smaller absorption and birefringence that is favorable for collinear PM [32]. However, susceptibility to photochromic damage under high-intensity pumping, known as gray- or grey-tracking could be its disadvantage [1].

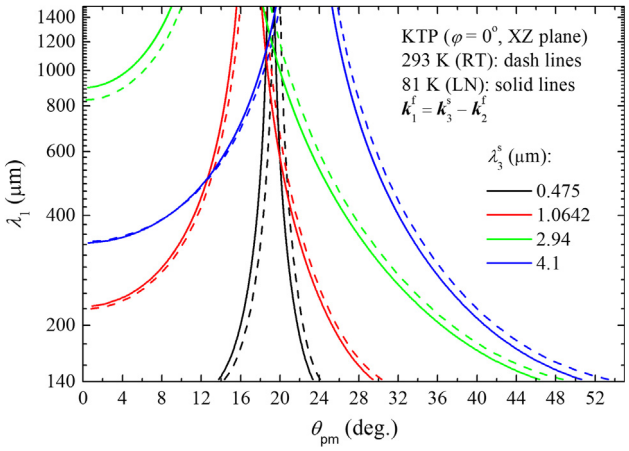

Fig. 6. Phase-matching curves for $s-f \rightarrow f$ type down-conversion of THL − 100 (λ = 0.475 μm, black lines) [23], Nd:YAG (1.064 μm, red), Er:YAG (2.94 μm, green), DF (4.1 μm, blue) lasers and close-wavelength emission into the THz domain in the first quadrant of KTP crystal at 293 K and 81 K vs. θ and φ angles. (For interpretation of the references to colour in this figure legend, the reader is referred to the web version of this article.)

4. Conclusion

In conclusion, we present optical properties of high optical quality flux-grown KTP crystals studied by the time-domain spectroscopy for THz waves polarized parallel to all three optical axes in the range of 0.2–2.4 THz at 81 K and compare them to room temperature results. Absorption coefficients α_x and α_y at 81 K a few times lower to that of widely used GaSe crystal and $LiNbO_3$ crystals, and do not have any strong phonon peaks at the frequencies below 2.15 THz. All the absorption coefficients decrease dramatically with the cooling down to 81 K that should lead to a significant increase in the potential frequency conversion efficiency. Dispersion of refractive index components at 81 K is approximated in the form of Sellmeier equations. By using the equations, it is found that KTP crystal has PM for DFG in the THz range almost in the entire transparency range in the THz domain and in the favorable principle ***XZ***-plane. Moreover, for the first time, it is found that phase-matched SHG of a THz wave is possible. PM demonstrates high thermal stability (insensitivity to the temperature variation) like that in the main transparency window. Thus, low absorption at visible, IR and THz wavelengths, PM for three-wave interactions together with the exceptional set of known physical properties render KTP crystals amongst the most prospective crystals for high-power THz wave generation. Growth technology available for producing cm-sized KTP

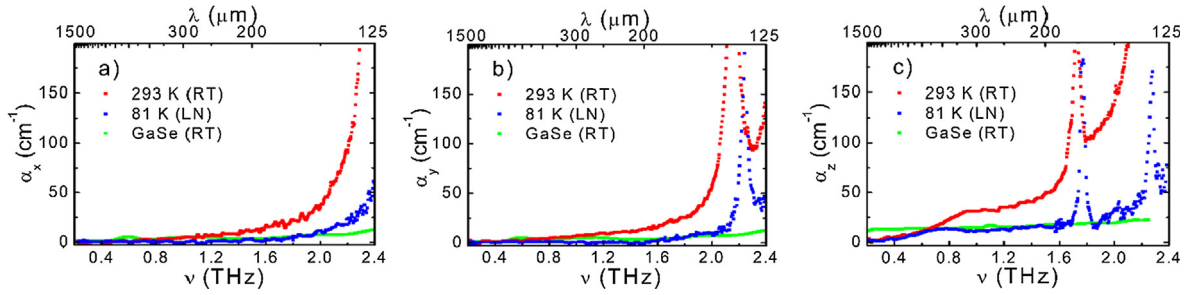

Fig. 5. Absorption coefficient spectra of three axes of KTP crystal at 293 K and 81 K. GaSe absorption was adopted from [10] for comparison.

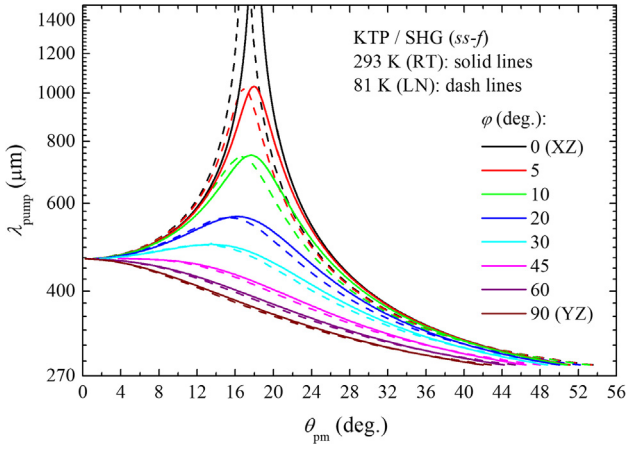

Fig. 7. SHG phase-matching curves for THz waves in the first quadrant of KTP at 293 K and 81 K.

crystals also seems important for THz applications.

Conflicts of interest

We have no conflicts of interest to declare.

Acknowledgements

The study was financially supported by National Key Research and Development Program of China, China, No. 2016YFE0120200 and Foundation of Youth Innovation Promotion Association of the Chinese Academy of Sciences, China, No. 2017259 (model study); Russian Foundation for Basic Research (RFBR), Russia, Project #17-32-80039 (experimental study). The terahertz spectroscopy measurements were carried out on the THz-TDS at the Shared Equipment Centre "Spectroscopy and Optics" of the Institute of Automation and Electrometry SB RAS, Novosibirsk, Russia

References

[1] D. Nikogosyan, Nonlinear Optical Crystals: A Complete Survey, Springer, New York, 2005 (accessed October 18, 2017), https://www.springer.com/gp/book/9780387220222.

[2] A.H. Reshak, I.V. Kityk, S. Auluck, Investigation of the linear and nonlinear optical susceptibilities of $KTiOPO_4$ single crystals: theory and experiment, J. Phys. Chem. B 114 (2010) 16705–16712, https://doi.org/10.1021/jp1072878.

[3] K. Vivekanandan, S. Selvasekarapandian, P. Kolandaivel, M.T. Sebastian, S. Suma, Raman and FT-IR spectroscopic characterisation of flux grown $KTiOPO_4$ and $KRbTiOPO_4$ non-linear optical crystals, Mater. Chem. Phys. 49 (1997) 204–210, https://doi.org/10.1016/S0254-0584(97)80165-4.

[4] J.T. Lin, J.L. Montgomery, Generation of tunable mid-IR (1.8–2.4 μm) laser from optical parametric oscillation in KTP, Opt. Commun.. 75 (1990) 315–320, https://doi.org/10.1016/0030-4018(90)90539-6.

[5] G.C. Bhar, A.M. Rudra, A.K. Chaudhary, T. Sasaki, Y. Mori, Highly efficient difference-frequency generation in KTP, Appl. Phys. B Laser Opt. 63 (1996) 141–144, https://doi.org/10.1007/BF01095264.

[6] G.C. Bhar, U. Chatterjee, A.M. Rudra, A.K. Chaudhary, Generation of widely tunable mid-infrared radiation by difference frequency mixing in KTP, J. Phys. D Appl. Phys. 30 (1997) 2693–2697, https://doi.org/10.1088/0022-3727/30/19/006.

[7] P. Mounaix, L. Sarger, J.P. Caumes, E. Freysz, Characterization of non-linear potassium crystals in the terahertz frequency domain, Opt. Commun. 242 (2004) 631–639, https://doi.org/10.1016/j.optcom.2004.08.043.

[8] M. Sang, L. Fan, X. Lu, W. Zhang, Optical phonon resonance of $KTiOPO_4$ crystal characterized by THz time-domain spectroscopy, Acta Photonica Sinica. 32 (2009) 1286–1290.

[9] V.D. Antsygin, A.B. Kaplun, A.A. Mamrashev, N.A. Nikolaev, O.I. Potaturkin, Terahertz optical properties of potassium titanyl phosphate crystals, Opt. Exp. 22 (2014) 25436, https://doi.org/10.1364/OE.22.025436.

[10] J.F. Molloy, M. Naftaly, Yu. Andreev, K. Kokh, G. Lanskii, V. Svetlichnyi, Absorption anisotropy in sulfur doped gallium selenide crystals studied by THz-TDS, Opt. Mater. Exp. 4 (2014) 2451–2459, https://doi.org/10.1364/OME.4.002451.

[11] J. Guo, J.-J. Xie, D.-J. Li, G.-L. Yang, F. Chen, C.-R. Wang, L.-M. Zhang, Y.M. Andreev, K.A. Kokh, G.V. Lanskii, V.A. Svetlichnyi, Doped GaSe crystals for laser frequency conversion, Light Sci. Appl. 4 (2015) e362, https://doi.org/10.1038/lsa.2015.135.

[12] W. Wang, Z. Cong, X. Chen, X. Zhang, Z. Qin, G. Tang, N. Li, C. Wang, Q. Lu, Terahertz parametric oscillator based on $KTiOPO_4$ crystal, Opt. Lett. 39 (2014) 3706, https://doi.org/10.1364/OL.39.003706.

[13] M.-H. Wu, Y.-C. Chiu, T.-D. Wang, G. Zhao, A. Zukauskas, F. Laurell, Y.-C. Huang, Terahertz parametric generation and amplification from potassium titanyl phosphate in comparison with lithium niobate and lithium tantalate, Opt. Exp. 24 (2016) 25964, https://doi.org/10.1364/OE.24.025964.

[14] T.A. Ortega, H.M. Pask, D.J. Spence, A.J. Lee, Stimulated polariton scattering in an intracavity $RbTiOPO_4$ crystal generating frequency-tunable THz output, Opt. Exp. 24 (2016) 10254, https://doi.org/10.1364/OE.24.010254.

[15] J. Shikata, M. Sato, T. Taniuchi, H. Ito, K. Kawase, Enhancement of terahertz-wave output from $LiNbO_3$ optical parametric oscillators by cryogenic cooling, Opt. Lett. 24 (1999) 202, https://doi.org/10.1364/OL.24.000202.

[16] V.D. Antsygin, A.A. Mamrashev, N.A. Nikolaev, O.I. Potaturkin, T.B. Bekker, V.P. Solntsev, Optical properties of borate crystals in terahertz region, Opt. Commun. 309 (2013) 333–337, https://doi.org/10.1016/j.optcom.2013.08.014.

[17] A. Mamrashev, N. Nikolaev, V. Antsygin, Y. Andreev, G. Lanskii, A. Meshalkin, Optical properties of KTP crystals and their potential for terahertz generation, Crystals 8 (2018) 310, https://doi.org/10.3390/cryst8080310.

[18] V.A. Rusov, A.V. Gorchakov, A.L. Belostotsky, V.K. Sapojnikov, A.B. Kaplun, A.B. Meshalkin, V.N. Shapovalov, $KTiOPO_4$ electro-optical devices with extinction ratio up to 1:1000, Proceedings of SPIE, 2001, pp. 117–119, https://doi.org/10.1117/12.420953.

[19] Q. Wu, X.C. Zhang, Free-space electro-optics sampling of mid-infrared pulses, Appl. Phys. Lett. 71 (1997) 1285–1286, https://doi.org/10.1063/1.119873.

[20] A.A. Mamrashev, O.I. Potaturkin, Characteristics of the system of polarization-optical detection of a pulsed terahertz spectrometer, Optoelect. Instrument. Data Process. 47 (2011) 332–337, https://doi.org/10.3103/S8756699011040029.

[21] V.D. Antsygin, V.F. Losev, A.A. Mamrashev, N.A. Nikolaev, O.I. Potaturkin, Specific features of studying anisotropic media by methods of time-domain terahertz spectroscopy, Optoelect. Instrument. Data Process. 52 (2016) 374–380, https://doi.org/10.3103/S8756699016040099.

[22] L. Duvillaret, F. Garet, J.-L. Coutaz, J.F. Whitaker, A reliable method for the extraction of material parameters of thick and thin samples in THz time-domain spectroscopy, Ultrafast Electronics and Optoelectronics (1997), Paper UF10, Optical Society of America, 1997, p. UF10 (accessed July 31, 2018), https://www.osapublishing.org/abstract.cfm?uri=UEO-1997-UF10.

[23] N.G. Kononova, A.E. Kokh, K.A. Kokh, G.V. Lanskii, V.F. Losev, V.A. Svetlichnyi, Y.M. Andreev, Down-conversion of short-wavelength radiation in LBO crystal, Russ. Phys. J. 59 (2016) 1307–1315, https://doi.org/10.1007/s11182-016-0907-4.

[24] V.D. Zvorykin, N.V. Didenko, A.A. Ionin, I.V. Kholin, A.V. Konyashchenko, O.N. Krokhin, A.O. Levchenko, A.O. Mavritskii, G.A. Mesyats, A.G. Molchanov, M.A. Rogulev, L.V. Seleznev, D.V. Sinitsyn, S.Y. Tenyakov, N.N. Ustinovskii, D.A. Zayarnyi, GARPUN-MTW: A hybrid Ti:Sapphire/KrF laser facility for simultaneous amplification of subpicosecond/nanosecond pulses relevant to fast-ignition ICF concept, Laser Part. Beams 25 (2007), https://doi.org/10.1017/S0263034607000559.

[25] J.-G. Huang, Z.-M. Huang, N.A. Nikolaev, A.A. Mamrashev, V.D. Antsygin, O.I. Potaturkin, A.B. Meshalkin, A.B. Kaplun, G.V. Lanskii, Y.M. Andreev, D.M. Ezhov, V.A. Svetlichnyi, Phase matching in RT KTP crystal for down-conversion into the THz range, Laser Phys. Lett. 15 (2018) 075401, https://doi.org/10.1088/1612-202X/aabb30.

[26] K. Kato, E. Takaoka, Sellmeier and thermo-optic dispersion formulas for KTP, Appl. Opt. 41 (2002) 5040–5044, https://doi.org/10.1364/AO.41.005040.

[27] B. Wyncke, F. Brehat, J. Mangin, G. Marnier, M.F. Ravet, M. Metzger, Infrared reflectivity spectrum of $KTiOPO_4$ single crystal, Phase Transitions 9 (1987) 179–183, https://doi.org/10.1080/01411598708240782.

[28] G.E. Kugel, F. Brehat, B. Wyncke, M.D. Fontana, G. Marnier, C. Carabatos-Nedelec, J. Mangin, The vibrational spectrum of a $KTiOPO_4$ single crystal studied by Raman and infrared reflectivity spectroscopy, J. Phys. C: Solid State Phys. 21 (1988) 5565, https://doi.org/10.1088/0022-3719/21/32/011.

[29] Y.M. Andreev, M. Naftaly, J.F. Molloy, A.E. Kokh, G.V. Lanskii, V.A. Svetlichnyi, V.F. Losev, N.G. Kononova, K.A. Kokh, LBO: optical properties and potential for THz application, Laser Phys. Lett. 12 (2015) 115402, https://doi.org/10.1088/1612-2011/12/11/115402.

[30] D.M. Lubenko, V.F. Losev, Y.M. Andreev, G.V. Lanskii, Model studies of THz-range generation via down conversion of the radiation of Ti: sapphire lasers in LBO crystals, Bulletin Russian Academy Sci.: Phys. 81 (2017) 1239–1243, https://doi.org/10.3103/S1062873817100185.

[31] G.G. Gurzadyan, V.G. Dmitriev, D.N. Nikogosyan, Handbook of Nonlinear Optical Crystals, 3rd ed., Springer, Berlin; New York, 1999.

[32] M.C. Hoffmann, J.A. Fülöp, Intense ultrashort terahertz pulses: generation and applications, J. Phys. D Appl. Phys. 44 (2011) 083001, https://doi.org/10.1088/0022-3727/44/8/083001.